Journal of Computational Mathematics and Data Science 1 (2021) 100014

Contents lists available at ScienceDirect

Journal of Computational Mathematics and Data Science

journal homepage: www.elsevier.com/locate/jcmds

Efficient adaptive exponential time integrators for nonlinear Schrödinger equations with nonlocal potential

Winfried Auzinger [a], Iva Březinová [b], Alexander Grosz [g], Harald Hofstätter [a], Othmar Koch [c,*], Takeshi Sato [d,e,f]

[a] Institute of Analysis and Scientific Computing, TU Wien, Wiedner Hauptstraße 8-10, 1040 Wien, Austria
[b] Institute of Theoretical Physics, TU Wien, Wiedner Hauptstraße 8-10, 1040 Wien, Austria
[c] Institut für Mathematik, Universität Wien, Oskar-Morgensternplatz 1, 1090 Wien, Austria
[d] Department of Nuclear Engineering and Management, University of Tokyo, 7-3-1 Hongo, Bunkyo-ku, Tokyo, 113-8656, Japan
[e] Photon Science Center, Graduate School of Engineering, The University of Tokyo, 7-3-1 Hongo, Bunkyo-ku, Tokyo 113-8656, Japan
[f] Research Institute for Photon Science and Laser Technology, The University of Tokyo, 7-3-1 Hongo, Bunkyo-ku, Tokyo, 113-0033, Japan
[g] Department of Mathematics, Technical University of Munich, Arcisstraße 21, D-80333 München, Germany

ARTICLE INFO

MSC:
65M20
65M50
65M70
81-08

Keywords:
Multiconfiguration time-dependent Hartree–Fock method
Splitting methods
Exponential integrators
Lawson methods
Local error estimators
Adaptive stepsize selection

ABSTRACT

The performance of exponential-based numerical integrators for the time propagation of the equations associated with the multiconfiguration time-dependent Hartree–Fock (MCTDHF) method for the approximation of the multi-particle Schrödinger equation in one space dimension is assessed. Among the most popular integrators such as Runge–Kutta methods, time-splitting, exponential integrators and Lawson methods, exponential Lawson multistep methods with one predictor–corrector step provide the best stability and accuracy at the least effort. This assessment is based on the observation that the evaluation of the nonlocal terms associated with the potential is the computationally most demanding part of such a calculation in our setting. In addition, the predictor step provides an estimator for the local time-stepping error, thus allowing for adaptive time-stepping which reflects the smoothness of the solution and enables to reliably control the accuracy of a computation in a robust way, without the need to guess an optimal stepsize a priori. One-dimensional model examples are studied to compare different time integrators and demonstrate the successful application of our adaptive methods.

1. Introduction and overview

We benchmark time integration schemes for nonlinear Schrödinger equations of the form

$$\partial_t u(t) = Au(t) + B(u(t)), \quad t > t_0, \qquad u(t_0) = u_0, \tag{1.1}$$

on a Hilbert space $\mathscr{H}$. Here, $A : \mathscr{D} \subseteq \mathscr{H} \to \mathscr{H}$ is a self-adjoint differential operator and B a generally unbounded nonlinear operator.

Such equations often arise in the context of model reductions for high-dimensional quantum dynamical systems and serve to make high-dimensional quantum simulations computationally tractable, see for instance [1–6].

Our main interest is in the equations of motion arising in the MCTDHF approximation for multi-electron systems. In all the mentioned approaches evaluations of the nonlinear operator B are expensive to compute and thus, it is crucial that a

* Corresponding author.
E-mail addresses: winfried.auzinger@tuwien.ac.at (W. Auzinger), iva.brezinova@tuwien.ac.at (I. Březinová), alexander.grosz@tum.de (A. Grosz), hofi@harald-hofstaetter.at (H. Hofstätter), othmar@othmar-koch.org (O. Koch), sato@atto.t.u-tokyo.ac.jp (T. Sato).

https://doi.org/10.1016/j.jcmds.2021.100014
Received 1 August 2021; Received in revised form 8 November 2021; Accepted 11 November 2021
Available online xxxx

numerical method requires a minimal number of evaluations of this operator while retaining accuracy and stability also in long-time integration. Thus, our results also indicate promising directions for other fields. We mention that for particular spatial discretizations [6], the nonlocal terms can be evaluated economically at the cost of more expensive computations for the separable part A. This is, however, not our focus in this study.

In our one-dimensional setting, we impose periodic boundary conditions on a sufficiently large interval, a corresponding spatial discretization by a Fourier pseudospectral method, and evaluate the meanfield integrals by the trapezoidal rule, which offers the special benefit of spectral convergence in this particular situation [7]. The propagation of A in our setting can thus be facilitated essentially at the cost of two transforms between real and frequency space, which are cheap to compute. Indeed, it was demonstrated already in [8] that the computation time and the number of evaluations of B are proportional, see also Section 3 below.

Diverse approaches for the numerical approximation of quantum dynamical systems have been discussed by different authors. These are comprehensively discussed for instance in [9]. The accuracy and efficiency of splitting methods has been demonstrated for various quantum mechanical models under a number of different spatial discretizations, see for instance [10–12] and references therein. In the present work, however, it is found that high-order splitting methods are less efficient for our purpose than high-order multistep approaches, but they still represent a viable choice as they show a very stable behavior.

An important aspect that we consider is long-time integration of the MCTDHF equations. Long integration times are for instance required for the detection of Anderson localization in an expanding Bose–Einstein condensate [13]. Stability of the numerical time integration is thus a crucial aspect, which we investigate by monitoring norm conservation of the numerical approximation. A method which cannot provide this most elementary property on a sufficiently long time interval cannot be used for our purpose and is thus ruled out from further considerations, see Sections 3.1 and 3.2 below.

Our emphasis is on adaptive choice of the time-steps based on asymptotically correct estimators of the local error. We will demonstrate that this has the potential to increase the efficiency of the computations. We stress that a very important benefit of adaptive error control is the possibility to obtain reliable information on the achieved accuracy of a simulation instantaneously. In this way, it is not necessary to guess a priori a suitable stepsize and repeat a calculation if the results are unsatisfactory, and the results can be trusted within the prescribed tolerance.

1.1. Splitting methods

Popular integrators for Schrödinger equations are exponential time-splitting methods based on multiplicative combinations of the partial flows of A and B, where the coefficients in this composition are determined such that a prescribed order of consistency is obtained [14]. At the (time-)semi-discrete level, s-stage exponential splitting methods for the integration of (1.1) use the partial flows $\mathscr{E}_A(t,u_0) : u_0 \mapsto u(t) = \mathrm{e}^{tA}u_0$ and $\mathscr{E}_B(t,u_0) : u_0 \mapsto u(t)$ with $u'(t) = B(u(t)),\ u(0) = u_0$. For a single step $(t_n,u_n) \mapsto (t_{n+1},u_{n+1})$ with time step h, this reads

$$u_{n+1} := \mathscr{S}(h,u_n) = \mathscr{E}_B(b_s h,\cdot)\circ\mathscr{E}_A(a_s h,\cdot)\circ \ldots \circ\mathscr{E}_B(b_1 h,\cdot)\circ\mathscr{E}_A(a_1 h,u_n), \tag{1.2}$$

where the coefficients $a_j, b_j,\ j = 1 \ldots s$ are determined according to the requirement that a prescribed order of consistency is obtained [14].

The first rigorous mathematical error analysis for low order splitting methods applied to linear Schrödinger equations was conducted in [15]. An extension to higher-order schemes is provided by [16]. The nonlinear setting was first analyzed for the second-order Strang splitting in [17], see also [18], and a convergence proof for high-order methods which also covers the equations of motion associated with MCTDHF is given in [19]. In the present study, we will use splittings constructed by the composition approaches by Suzuki and Yoshida, respectively, see [14], to obtain fourth order integrators, and the popular second-order Strang splitting for comparison. In the figures in Section 3, we will use the following abbreviations for the investigated schemes. The Strang splitting, where B is propagated by the explicit second order Runge–Kutta method by Heun, is denoted as `Strang (RK2)`, the Suzuki splitting, where B is propagated by the classical fourth-order Runge–Kutta method, is `Suzuki (RK4)`, propagation by the midpoint rule with three fixed point iterations corresponds with `Suzuki (MP with 3 it.)`, and similarly for the Yoshida splitting `Yoshida`.

1.2. Exponential integrators

An approach which also exploits a different treatment of the two vector fields is given by the class of exponential integrators [20,21]. Here, the variation of constant formula (VOC) is used to separate the two given vector fields and the arising integral is subsequently suitably approximated. Exponential integrators are comprehensively discussed in the two reviews [22,23]. A first preliminary study of their performance for the MCTDHF equations was conducted in [8].

In this approach, the solution of (1.1) for a time-step $t_n \to t_{n+1} = t_n + h$ is expressed as the solution of

$$u(t_n + h) = \mathrm{e}^{hA}u_n + \int_0^h \mathrm{e}^{(h-\tau)A}B(u(t_n+\tau))\,\mathrm{d}\tau. \tag{1.3}$$

by the VOC. Different exponential-type integrators are distinguished depending on how the integral in (1.3) is approximated.

Exponential Runge–Kutta methods. When the integral in (1.3) is approximated by a quadrature formula of Runge–Kutta type, relying on evaluations of the nonlinear operator B at interior points $t_n + h\tau_j$, $\tau_j \in [0,1]$, $j = 1, \dots, k$, an *exponential Runge–Kutta* method is obtained. This corresponds to replacing $B(u(t_n + \tau))$ in the integrand by a polynomial interpolant at the points

$$(t_n + h\tau_1, B(u(t_n + h\tau_1))), \dots, (t_n + h\tau_k, B(u(t_n + h\tau_k))).$$

The method is realized by stepping from $t_n + h\tau_j \to t_n + h\tau_{j+1}$ in the same way as in a Runge–Kutta method for $\partial_t u = B(u)$, with appropriately modified weights of the stages. For implicit methods, nonlinear systems of equations have to be solved, which is generally considered as prohibitively expensive and therefore not practically used. Note that after interpolation, the resulting integral can be evaluated analytically by using the φ-functions, see for example [24]. Such a procedure has first been proposed in [25] and analyzed for stiff problems in [26], see also [22].

The denotation *exponential integrator* first appeared in [21], where explicit exponential Runge–Kutta methods are considered. There, the non-stiff order conditions are derived, and fourth order methods are constructed along with reduced methods which promise significant computational advantages when used in conjunction with Krylov methods for approximating the matrix exponential. Also, stepsize control linked with the Krylov-substeps is proposed, and embedded Runge–Kutta methods serve as a basis for adjusting the time-step.

More recently, a systematic theory to derive the order conditions based on the variation of constant formula, and trees related to Faà di Bruno's formula, similarly as for classical Runge–Kutta methods, has been established in [27]. Studies of exponential Crank–Nicolson integrators in conjunction with Padé approximation of the matrix exponential were conducted in [28], which also gives a linear stability analysis and uses extrapolation to improve the basic order two. A comparative study of exponential integrators is given in [29] which seems to favor explicit exponential Runge–Kutta methods. An adaptive approach based on embedded pairs of formulae is also studied there. In the present paper, we use the fourth-order explicit exponential Runge–Kutta method by Krogstad, see [22,30], which in the figures in Section 3 we denote as `Krogstad`.

Exponential multistep methods. Alternatively, the integral in (1.3) can be approximated in terms of an interpolation polynomial at previous points

$$(-(k-1)h, B(u_{n-k+1})), \dots, (-h, B(u_{n-1})), (0, B(u_n)).$$

This yields an (explicit) exponential Adams–Bashforth type multistep method, see for instance [31,32]. If the interpolation also includes the forward point, that is, the interpolation comprises

$$(-(k-1)h, B(u_{n-k+1})), \dots, (-h, B(u_{n-1})), (0, B(u_n)), (h, B(u_{n+1})),$$

an (implicit) exponential Adams–Moulton type method is obtained. These two approaches can be combined in a predictor–corrector method in the same way as for conventional linear multistep methods.

Exponential multistep methods were first considered and analyzed in [31] under the assumption of smooth B. A starting strategy is also given there. A similar approach is adopted in [32], with a different integration domain in the variation of constant formula, and a linearized version is proposed. The stability analysis proceeds as in [33]. Related exponential integrators of a multistep flavor are also considered in [34,35]. In the figures in Section 3, we denote exponential multistep methods by `Exponential multistep` k `steps with` j `P/C it.`, when the length of the method is k and j corrector steps are performed (j is either 0 or 1).

Lawson methods. In Lawson methods, the substitution

$$u(t) \to \mathrm{e}^{-tA} u(t) =: v(t) \tag{1.4a}$$

is applied to Eq. (1.1) ex ante. The resulting equation

$$v'(t) = \mathrm{e}^{-tA} B(\mathrm{e}^{tA} v(t)), \tag{1.4b}$$

can subsequently be solved by any appropriate time-stepping method.

The main advantage of the Lawson transformation lies in the fact that the dynamics associated with the non-smooth operator A is separated by the transformation (1.4a), while the problem (1.4b) subjected to the time-stepping scheme is smoother, thus allowing for larger time-steps. In practice, the space discretization is preferably chosen such that the resulting application of $\exp(\pm tA)$ is computationally cheap to realize. For instance, Fourier pseudospectral methods exploit the fact that the discretization of A is diagonal in frequency space if A is (a scalar multiple of) the Laplacian, which is the case for Schrödinger-type equations.

The Lawson transformation was first introduced in [36] for the ODE case, where Runge–Kutta methods were applied to the transformed problem and a classical non-stiff error analysis was applied to the resulting equation. Explicit multistep methods within the Lawson approach were introduced in [30]. In [37], explicit Lawson Runge–Kutta methods for the cubic nonlinear Schrödinger equation compare favorably with splitting and other methods. [38] studies mathematical features of the Lawson explicit fourth order Runge–Kutta method from [37] and gives an error analysis. The recently published article [39] gives a convergence proof for Lawson Runge–Kutta methods in the stiff case, however under the assumption that the operator B is smooth, which is not the case in the MCTDHF equations we are considering.

Adaptive choice of the time-steps in the context of Lawson methods has been considered in several papers. [40] compares error estimates based on mesh halving to the cheaper embedded Runge–Kutta methods [41], while in [42] projected Lawson Runge–Kutta methods are compared to splittings with embedded error estimators [43]. The method from [40] has been applied to the simulation

of light-wave propagation in optical fibers in [44]. A similar approach is adopted in [45], where adaptive time-stepping is favorable for the nonlinear Schrödinger equation.

In this paper, we will use the classical fourth-order Runge–Kutta method to solve the transformed equations, which we denote by `Lawson Runge-Kutta (RK4)` in the figures in Section 3.

Alternatively, we can view the Lawson approach as an approximation to the representation (1.3), where, in contrast to standard exponential integrators, the whole integrand is replaced by a polynomial interpolant. To reduce the expensive evaluations of B, we focus on multistep methods. Exponential Lawson multistep methods are then constructed by replacing the integrand by an interpolant at

$$(-(k-1)h, \mathrm{e}^{(k-1)hA}B(u_{n-k+1})), \dots, (-h, \mathrm{e}^{hA}B(u_{n-1})), (0, B(u_n)), [(h, \mathrm{e}^{-hA}B(u_{n+1}))].$$

The last point in square brackets is used for implicit methods, while otherwise the methods are explicit.

This results in a finite difference method

$$u_{n+1} = \mathrm{e}^{hA}u_n + h\sum_{j=1}^{k}\beta_j \mathrm{e}^{(k-j+1)hA}B(u_{n-k+j})\ [+h\beta_{k+1}B(u_{n+1})], \quad n \geq k, \tag{1.5}$$

where the last term $[+h\beta_{k+1}B(u_{n+1})]$ appears in implicit Adams–Moulton type schemes and the values $u_0, \dots, u_{k-1}$ are obtained by a suitable auxiliary scheme ensuring order k. β_j, $j = 1, \dots, k+1$ are quadrature weights for $\int_0^h \mathrm{e}^{-\tau A}\pi(\tau)\,\mathrm{d}\tau$ resulting from the requirement that for polynomials π up to order k $[k+1]$, this integral should be reproduced exactly, see for instance [22]. This formulation is equivalent to the application of the corresponding linear multistep method to the transformed equation (1.4b). For the MCTDHF equations, an error analysis of Adams–Lawson multistep methods under minimal regularity assumptions is given in [46].

We will demonstrate that exponential Lawson multistep methods in a predictor–corrector implementation enhance stability of the numerical method for long-time integration, and also provide a local error estimator for adaptive time-stepping at no additional cost. High-order time propagators increase the efficiency. This does not imply additional computational cost in the multistep approach if no tight memory limitations have to be taken into account. Adaptive choice of the time-steps promises a further reduction in the computational effort. Note that this induces little additional work, since the error estimator is given by the predictor–corrector method which is used for stability reasons anyway. In the figures in Section 3, we will refer to these methods as `Adams-Lawson` k `steps with` j `P/C it.`, when the length of the formula is k and $j = 0/1$ corrector steps are performed.

Comparisons. To assess the performance of the exponential integration methods described above, we will also show results for the classical explicit Runge–Kutta method of fourth order (`RK4` in the figures in Section 3) and the second-order Strang splitting (used in conjunction with the second-order explicit Runge–Kutta method of Heun and denoted by `Strang (RK2)`), as these are popular integrators for quantum dynamics.

2. The MCTDHF method

In this paper we focus on the comparison of numerical methods applied to the equations associated with the multiconfiguration time-dependent Hartree–Fock method (MCTDHF) [3,47,48] for the time-dependent multi-particle Schrödinger equation

$$\mathrm{i}\frac{\partial\psi}{\partial t} = H\psi, \tag{2.1}$$

where the complex-valued *wave function* $\psi = \psi(x_1, \dots, x_f, t)$ depends on time t and, in the case considered here, the positions $x_1, \dots, x_f \in \mathbb{R}^3$ of electrons in an atom. The time-dependent Hamiltonian H is given as

$$\begin{aligned} H &= H(t) := \sum_{k=1}^{f}\Big(-\frac{1}{2}\Delta^{(k)} + U(x_k) + \sum_{\ell<k}V(x_k - x_\ell)\Big) + V_{\mathrm{ext}}(x_1, \dots, x_f, t) \\ &=: T + W(x_1, \dots, x_f, t), \\ T &= -\sum_{k=1}^{f}\frac{1}{2}\Delta^{(k)}, \quad U(x) = -\frac{Z}{|x|},\ Z \in \mathbb{N}, \quad V(x-y) = \frac{1}{|x-y|}. \end{aligned}$$

$V_{\mathrm{ext}}(x_1, \dots, x_f, t)$ represents a smooth external time-dependent potential, and $\Delta^{(k)}$ is the Laplace operator with respect to x_k only.

We recapitulate the MCTDHF method and implied equations of motion in the following. This serves to show the structure of the problems to be solved in order to corroborate our arguments about the computational demand of the numerical methods.

In MCTDHF as put forward in [3,47,48], the multi-electron wave function ψ from (2.1) is approximated in the manifold $\mathcal{M}$ of functions satisfying the ansatz

$$u = \sum_{(j_1,\dots,j_f)} a_{j_1,\dots,j_f}(t)\phi_{j_1}(x_1,t)\cdots\phi_{j_f}(x_f,t) =: \sum_J a_J(t)\Phi_J(x,t). \tag{2.2}$$

Using (2.2) for the *electronic* Schrödinger equation, the Pauli principle implies that only solutions u are considered which are antisymmetric under exchange of any two of their arguments x_j, x_k. This assumption implies antisymmetry in the coefficients, whence only $\binom{n}{f}$ equations for a_J have to be solved in the actual computations. This reduces the computational effort in the propagation of the operator A significantly.

The Dirac–Frenkel variational principle [49,50] in conjunction with gauging conditions is used to derive differential equations for the coefficients a_J and the orbitals ϕ_j in (2.2),

$$\mathrm{i}\,\frac{da_J}{dt} = \sum_K \langle \Phi_J\,|W|\,\Phi_K\rangle\, a_K, \quad \forall J, \tag{2.3a}$$

$$\mathrm{i}\,\frac{\partial \phi_j}{\partial t} = -\frac{1}{2}\Delta\phi_j + (I-P)\sum_{k=1}^{n}\sum_{l=1}^{n}\rho^{-1}_{j,l}\overline{W}_{l,k}\phi_k, \quad j=1,\dots,n, \tag{2.3b}$$

where

$$\psi_j := \langle \phi_j | u\rangle, \tag{2.4a}$$

$$\rho_{j,l} := \langle \psi_j | \psi_l\rangle, \tag{2.4b}$$

$$\overline{W}_{j,l} := \langle \psi_j\,|W|\,\psi_l\rangle, \tag{2.4c}$$

and P is the orthogonal projector onto the space spanned by the functions ϕ_j.

In our tests in one space dimension, we impose periodic boundary conditions and evaluate all occurring integrals by the trapezoidal rule (which amounts to simply summing up the values of the integrand on the chosen equidistant spatial grid). Nota bene, for periodic boundary conditions, this quadrature features optimal convergence properties [7, Section 3.3].

Clearly, the evaluation of (2.4b), (2.4c) causes most of the computational effort in our setting, and the number of evaluations of $\overline{W}$ should be kept to a minimum. We will henceforth denote

$$A = \frac{\mathrm{i}}{2}\left(0, \Delta^{(1)}, \dots, 0, \Delta^{(n)}\right)^T, \quad B = B(a,\phi), \tag{2.5}$$

where $a = (a_J)_J$ is the coefficient tensor and $\phi = (\phi_1,\dots,\phi_f)$. B represents the vector of the components associated with the potential, which constitute the computationally most expensive part.

3. Numerical comparisons

We will assess the performance of the numerical methods by computing two different models, one for the 1D helium atom and one for a 1D quantum dot, and choosing the number of orbitals in the MCTDHF method as $n = 4$ and $n = 6$. Some results for $n = 8$ and $n = 10$ are additionally given in Section 3.11.

The choice of the number of orbitals is dictated by limited resources for the broad comparisons. Since we observe that the conclusions for the choice of the most appropriate integrators correspond for $n = 4$ and $n = 6$ and the structure of the equations is the same also for larger n, our conclusions are representative. The same applies to the time interval for our tests, which is chosen as sufficiently large such as to eliminate unstable time integrators. For the Adams–Lawson P/C method with four steps, we will give a long-time simulation run for a number of orbitals which approaches a converged MCTDHF approximation in Section 3.11 in order to demonstrate the validity of our conclusions. We stress, however, that our choice of n is also supported by observations in [48]. According to [48], for the problem (3.1) below, $n = 4$ "can already account for the essential physics" and for (3.2), $n = 6$ yields "satisfactory accuracy" of the approximation.

Computations for a stationary problem, which just reproduce the groundstate, show that several methods fail by far to preserve even the norm of the wave function and can therefore not be used in long-time simulations.

Afterwards, the computational effort is investigated as compared to the achieved accuracy in relation to a highly accurate numerical reference solution. The reference solution for helium was computed with a constant stepsize of $\Delta t = 0.5^{11} \approx 4.88\cdot 10^{-4}$, for the quantum dot we used 12000 steps on the interval $[0,70]$, i.e. $\Delta t \approx 5.83\cdot 10^{-3}$, which is smaller than the adaptively chosen stepsizes and thus provides a more accurate solution. Clearly, the computation time is proportional to the number of evaluations of the nonlocal operator B, since the transformations between real and frequency space are cheap and so is the exponentiation of the kinetic operator. This has been verified already in [8], and is corroborated in Fig. 3.17 below.

3.1. Stability for the helium atom

As a first example we consider the MCTDHF equations for the helium atom in one spatial dimension, with $f = 2$.

The Hamiltonian is defined as

$$H(t) = H_0 + (x_1 + x_2)\,\mathscr{E}(t), \tag{3.1a}$$

$$H_0 = -\frac{1}{2}(\partial^2_{x_1} + \partial^2_{x_2}) - \frac{2}{\sqrt{x_1^2+b^2}} - \frac{2}{\sqrt{x_2^2+b^2}} + \frac{1}{\sqrt{(x_1-x_2)^2+b^2}}, \tag{3.1b}$$

with a smoothed Coulomb potential with shielding parameter $b = 0.7408$, where the atom is irradiated by a short, intense, linearly polarized laser pulse

$$\mathscr{E}(t) = \mathscr{E}_0\, g(t)\sin(\omega t).$$

The peak amplitude is set to $\mathscr{E}_0 = 0.1894$, the frequency is $\omega = 0.1837$, and we define the envelope $g(t) = 1.2\exp\left(-5\cdot 10^{-4}\,(t - 6\pi/\omega)^2\right)$. The parameters are taken from [48], and the envelope is a smooth approximation of the trapezoidal envelope chosen there. The

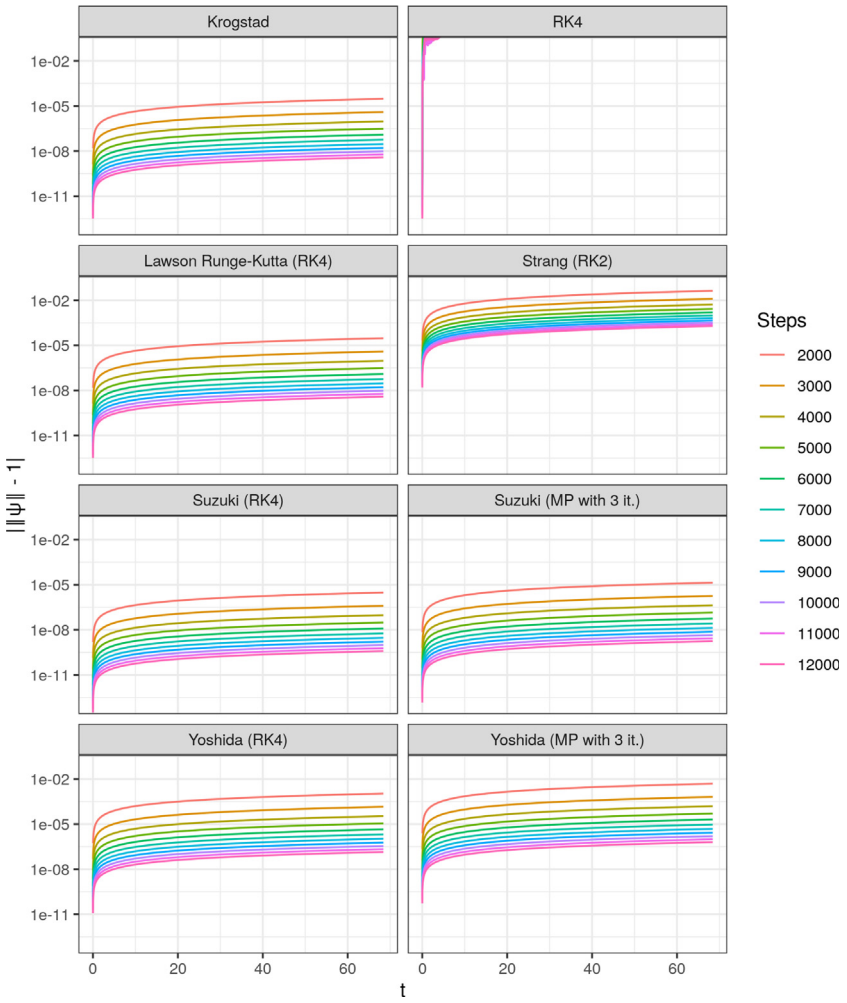

Fig. 3.1. Deviation from unit norm for the helium atom, MCTDHF with $n = 4$. One-step methods.

time integration proceeds for $t \in [0, 4\pi/\omega]$, which is sufficient to demonstrate the instability of the unsuitable schemes. Our choice of the integration time corresponds with 2 cycles of the laser pulse, while in [48] 6 cycles are computed. The longer integration time is considered for the purpose of illustration in Section 3.11 below.

In [48], this model serves to illustrate the effect of correlation on the probability density along the diagonal $x = y$, which implies that the single-configuration Hartree–Fock approximation is insufficient. We adopt a spin-restricted treatment (see [4]), where the number of space orbitals in the MCTDHF method is chosen as $n = 4$ in order to reduce the computation times for our extensive comparisons. The structure of the equations is the same also for larger n, therefore the conclusion about the most appropriate integrators remains valid also for larger n.

To investigate stability, we choose the interval $x \in [-16, 16]$, and a pseudospectral space discretization with 512 Fourier modes, and use equidistant time-steps, which are consistently refined. The number of time-steps in the given interval $t \in [0, 4\pi/\omega]$ is varied between 2000 and 12000 steps (see the legends of the graphs).

By observing the accuracy that the unitarity of the solution is preserved with in Figs. 3.1 and 3.2, it is clear that some of the time integrators which are popularly used for this type of quantum dynamics problems are not suitable in our context. The explicit fourth-order Runge–Kutta method (RK4) is stable only for excessively small time-steps, and exponential multistep methods are not stable either. Exponential one-step methods are stable for this problem, and so are splitting methods. In the realization of the splitting methods of composition type we are using here, it should be noted that the B-part can be propagated by the midpoint-rule with three fixed point iterations for the nonlinear equations, or alternatively by RK4. Both approaches have equal computational effort and also comparable accuracy, see Fig. 3.6. Exponential multistep methods perform unsatisfactorily in this experiment. In conjunction with the Lawson transformation, however, exponential one-step and multistep methods show satisfactory stability.

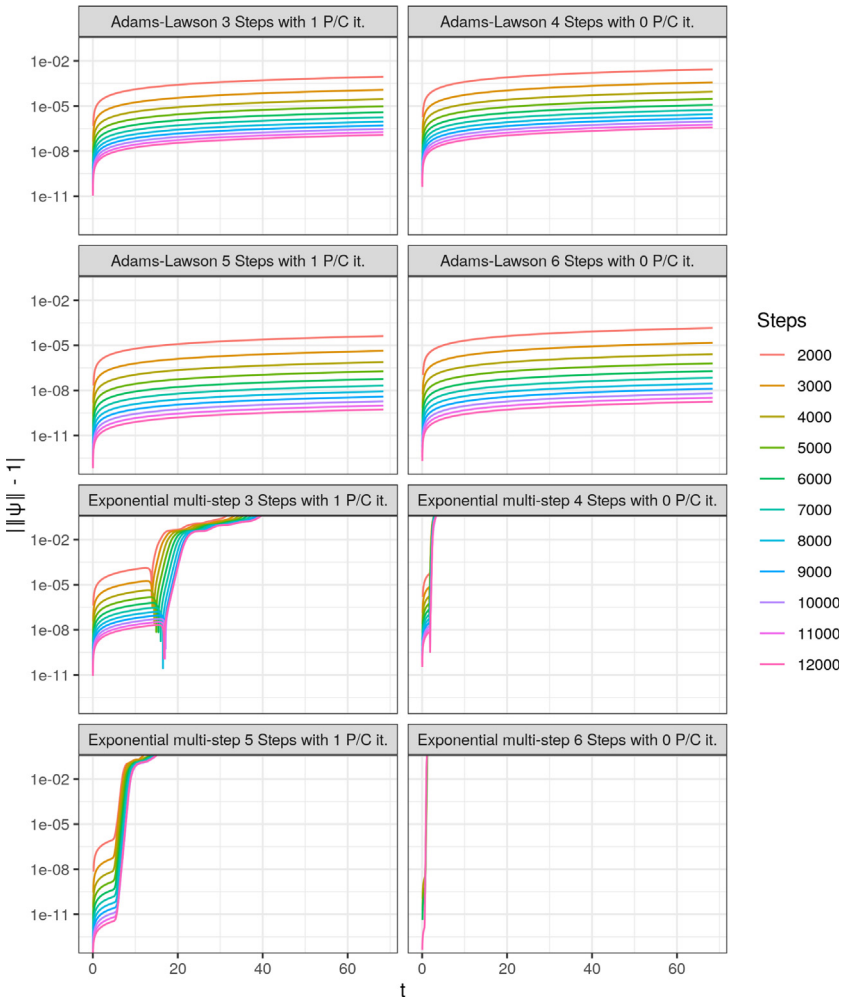

Fig. 3.2. Deviation from unit norm for the helium atom, MCTDHF with $n = 4$. Multistep methods.

3.2. Stability for the quantum dot

The second example we consider is a model of the one-dimensional quantum dot given by

$$H(t) = -\frac{1}{2}(\partial_{x_1}^2 + \partial_{x_2}^2) + \frac{1}{2}\Omega^2(x_1^2 + x_2^2) + \frac{1}{\sqrt{(x_1 - x_2)^2 + a^2}} + (x_1 + x_2)\mathscr{E}_0 \sin(\omega t), \tag{3.2}$$

with $\Omega = \frac{1}{4} = a, \mathscr{E}_0 = 1,\ \omega = 8\Omega = 2$, see [48]. The time interval is chosen as $t \in [0, 70]$ to eliminate methods unsuitable for long-time integration, and the spatial interval $x \in [-20, 20]$ is discretized with 1024 Fourier modes. For MCTDHF, here we use $n = 6$. Note that in [48], a much shorter time interval with $t_{\text{end}} \approx 12.5$ is used. Hence, in the subsequent investigations of convergence and efficiency, $t_{\text{end}} = 12$ will be used.

The stability is again investigated by monitoring the deviation from unit norm on the integration interval, see Figs. 3.3 and 3.4.

The conclusions from this experiment are analogous to the helium experiment. Among the methods that worked in a stable way for the helium experiment, however, for the quantum dot the sixth-order Adams–Lawson multistep method without a corrector step is found to be unstable, so this will also not be considered further.

3.3. Convergence for the helium atom

We now systematically investigate the error achieved by the different methods as compared to the computational effort. This is measured in terms of the evaluations of the nonlocal potential term B as this dominates the computational effort. It has been demonstrated already in [8] that, indeed, computation time and the number of evaluations of B are parallel and admit the same conclusions, see also Fig. 3.17 computed for the quantum dot in Section 3.8.

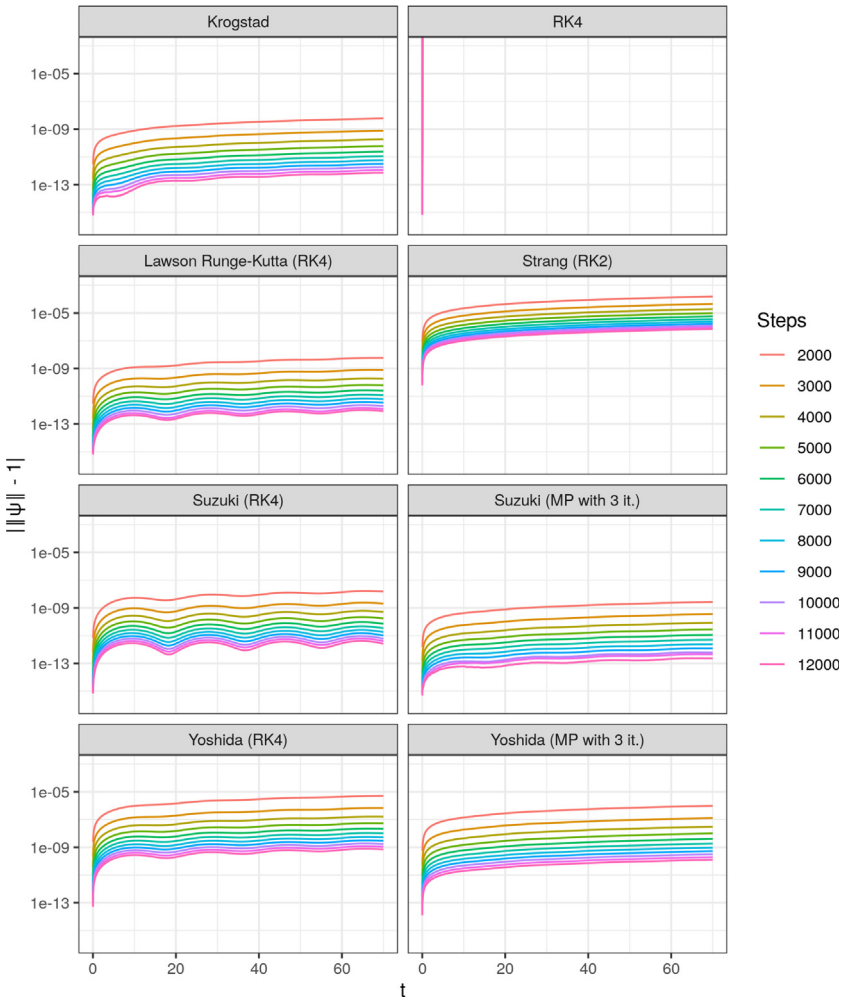

Fig. 3.3. Deviation from unit norm for the quantum dot, MCTDHF with $n = 6$. One-step methods.

We solve the MCTDHF equations with $n = 4$ for the helium atom (3.1) for the longer time interval $t \in [0, 80]$, and the spatial interval $x \in [-256, 256]$ is discretized with 8192 Fourier modes. In this first investigation, all the methods are propagated on equidistant time grids. The reason is that for one-step methods, error estimation has not been implemented due to the expectedly high additional computational effort for a local error estimator in the absence of specially constructed schemes. More importantly, we find that high-order multistep methods are more efficient even for constant stepsizes, so the cheap error estimation will be an additional bonus. The error as compared to the stepsize is given in Fig. 3.5, where the error is measured as the difference $\|u - u_{\text{ref}}\|$ in a discrete L^2 norm of the approximate solution tensor u and a reference solution u_{ref} on the same spatial grid. At accuracies of about 10^{-9}, some of the methods show an order reduction, which is likely to be attributed to limited spatial resolution.

The relation between the error and the number of evaluations of B is displayed in Fig. 3.6. We observe that the methods of highest order have the highest accuracy and also computational efficiency. The sixth-order Adams–Lawson method is stable only for very small time-steps, which is commensurate with the findings in Section 3.1, but efficient in this regime. The Adams–Lawson predictor/corrector method shows an order reduction for very high accuracies, but is nonetheless the most efficient stable integrator.

Among the splitting methods, clearly the Suzuki composition should be favored over the Yoshida composition.

Overall, it is clear that high-order Adams–Lawson methods with corrector step are the integrators that offer an optimal balance of stability and efficiency in the helium experiment, while in the absence of the corrector, methods of the comparable final order perform less favorably.[1] In this setting we conclude that a k-step method with one corrector step is more efficient than a $(k+1)$-step method without. Multistep methods without corrector step will therefore not be considered further.

[1] Observe that a multistep method with k steps has order k, with an additional corrector step, the order increases to $k+1$. Therefore, it is fair to compare the efficiency of methods with $k+1$ steps and no corrector step with k-step methods with one corrector step, as these have the same final order.

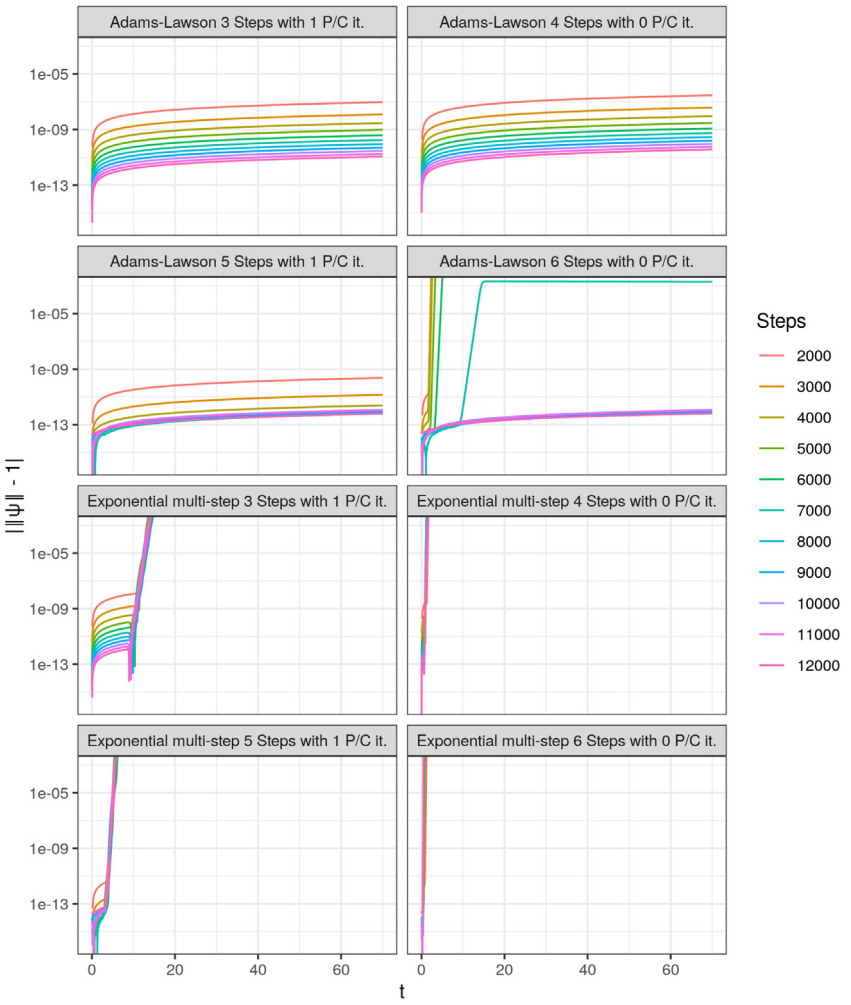

Fig. 3.4. Deviation from unit norm for the quantum dot, MCTDHF with $n = 6$. Multistep methods.

3.4. Convergence for the quantum dot

Next, we investigate the accuracy of the methods for the quantum dot, where $t \in [0, 12]$, $x \in [-20, 20]$, and the spatial discretization uses 1024 points. The time interval is similar to that in [48]. Fig. 3.7 shows the error as a function of the stepsize, and Fig. 3.8 as compared to evaluations of B.

For the quantum dot, all the methods show their expected convergence orders. While the error for high-order Lawson multistep methods is large for large stepsizes, the high order leads to the best efficiency for higher accuracies. Observe that while the Suzuki splitting method is very accurate for a given stepsize, the computational effort necessary for each step is detrimental for the efficiency. When the number of evaluations of B is considered, the Adams–Lawson methods are the most favorable, again the higher order multistep approach proves to be more efficient.

3.5. Efficiency of adaptive multistep methods for the helium atom

We next compare the different methods in a time-adaptive implementation for the computation of the helium atom, again for $t \in [0, 80]$, and $x \in [-256, 256]$ is discretized using 8192 Fourier modes. We adapt the time-step according to the standard strategy to satisfy a local error tolerance, see for instance [51,52]. We here consider exponential multistep and Adams–Lawson methods only. The reasons are the advantageous stability and convergence properties of the mentioned multistep methods.

We stress that the advantage of adaptive stepsize choice lies not only in the potential for increased efficiency when the smoothness of the solution varies over time, but more importantly in the reliable control of the solution's accuracy. Indeed, the computational effort for the evaluation of the error estimate is not always compensated for by the optimal choice of the local stepsize. However, an optimal equidistant stepsize cannot usually be guessed a priori, while adaptive stepsize selection automatically adapts the time-steps such that the prescribed error tolerance is satisfied. Hence, the accuracy of the numerical approximation is reliably controlled.

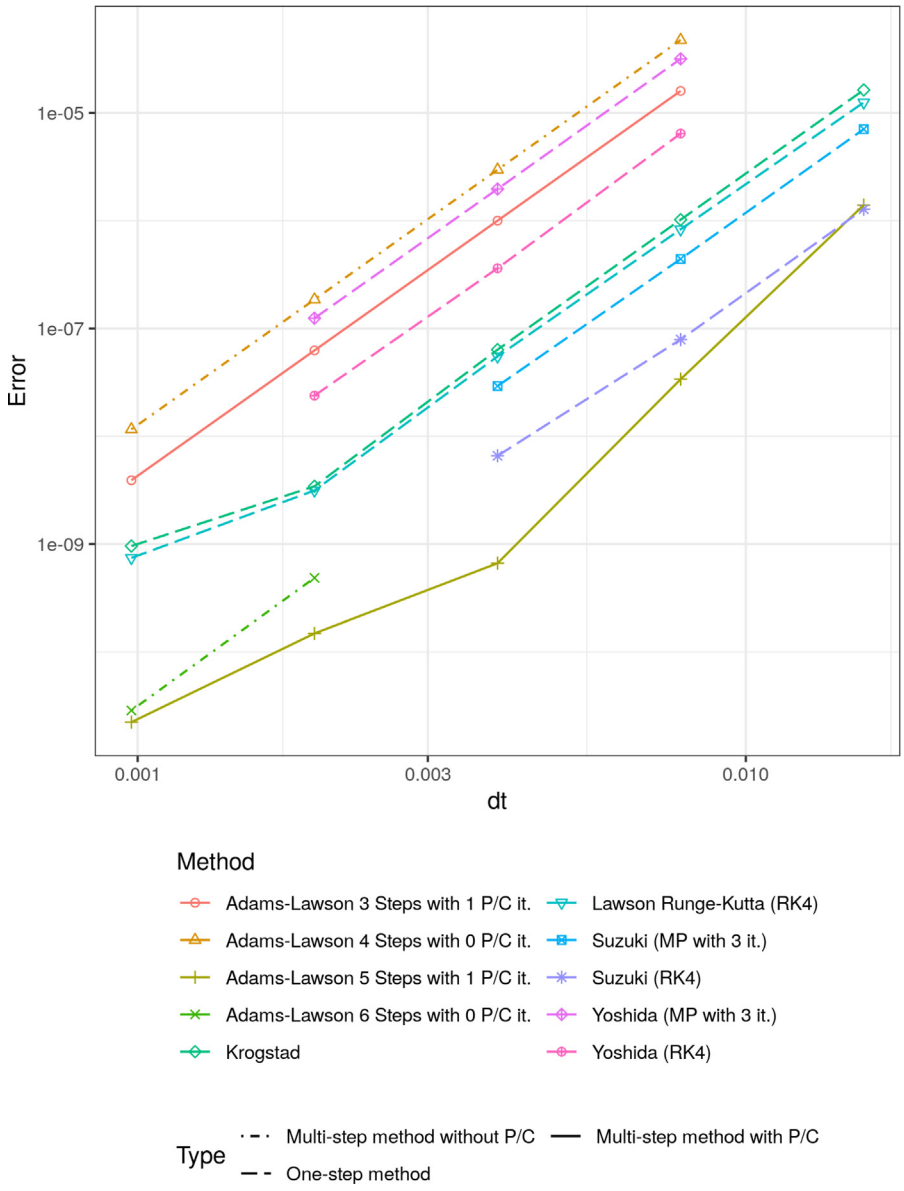

Fig. 3.5. Error by stepsize for the helium atom, MCTDHF with $n = 4$.

Fig. 3.9 gives the error as a function of the number of evaluations of B for helium approximated with $n = 4$ for Adams–Lawson methods of different orders, Fig. 3.10 gives the same information for exponential multistep methods. The methods of highest orders 7/8 no longer show a clear advantage over methods of orders 5/6 in all regimes of accuracy. This is to be attributed to a large error constant for the higher-order schemes. Thus, the method of order 5/6 seems to be the best choice. For comparison, the results are also shown for Lawson–Runge–Kutta and splitting methods on equidistant grids. Moreover, the multistep predictor/corrector method of length 5 (final order 6) is also shown on equidistant grids for the purpose of comparison. We observe that adaptive time-stepping with the same integrator shows comparable efficiency here, but provides reliable accuracy of the solution.

The exponential multistep methods show no systematic convergence behavior, which is commensurate with the observation that they are not stable. However, adaptive stepsize selection can still ensure that the stepsize is decreased to such an extent that the solution has acceptable accuracy. In the same stepsize regime, the Lawson and splitting methods are stable and show a systematic behavior, and display a clear advantage even for constant stepsizes. We note that the integrators with constant stepsizes show order reductions for very high accuracies, which is to be attributed to limitations in the accuracy related to the spatial resolution.

The attainable order in the time integration is influenced also by the spatial discretization error. This induces an unsystematic error which for high accuracies manifests itself as an order reduction in the last refinement step.

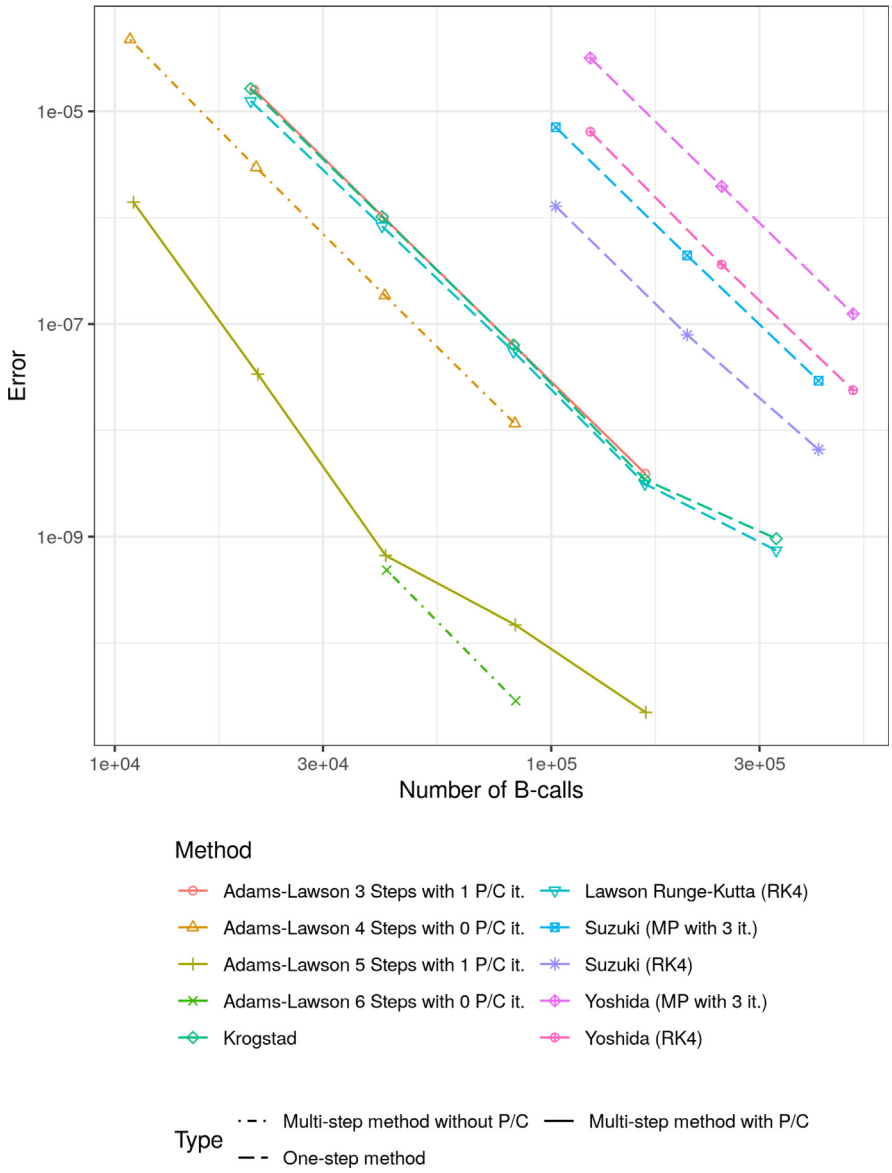

Fig. 3.6. Error by number of evaluations of B for the helium atom, MCTDHF with $n = 4$.

3.6. *Efficiency of adaptive multistep methods for the quantum dot*

We substantiate the comparisons of adaptive methods with additional results for the quantum dot, where as before $t \in [0, 12]$, $x \in [-20, 20]$, and 1024 Fourier modes are used. The observations on the properties of the methods are commensurate with those made in Section 3.5 for the helium atom, compare Figs. 3.9 and 3.11, and Figs. 3.10 and 3.12, respectively.

3.7. *Evolution of automatically chosen stepsizes*

In this section, we illustrate the stepsizes chosen automatically based on the error estimators provided by Adams–Lawson predictor/corrector methods. Fig. 3.13 shows the stepsizes chosen for several Lawson-multistep methods of different orders for the helium atom when a local error tolerance of 10^{-5} is prescribed, Fig. 3.14 shows the same for the quantum dot. We observe that stepsizes follow the smoothness of the energy functional, which serves as an indicator of the local solution smoothness. Encouragingly, stepsizes decrease where the solution varies more rapidly, and increase when smoothness of the solution is restored. Note that in the plots, the total energies computed by different numerical methods are graphically indistinguishable and obliterate each other.

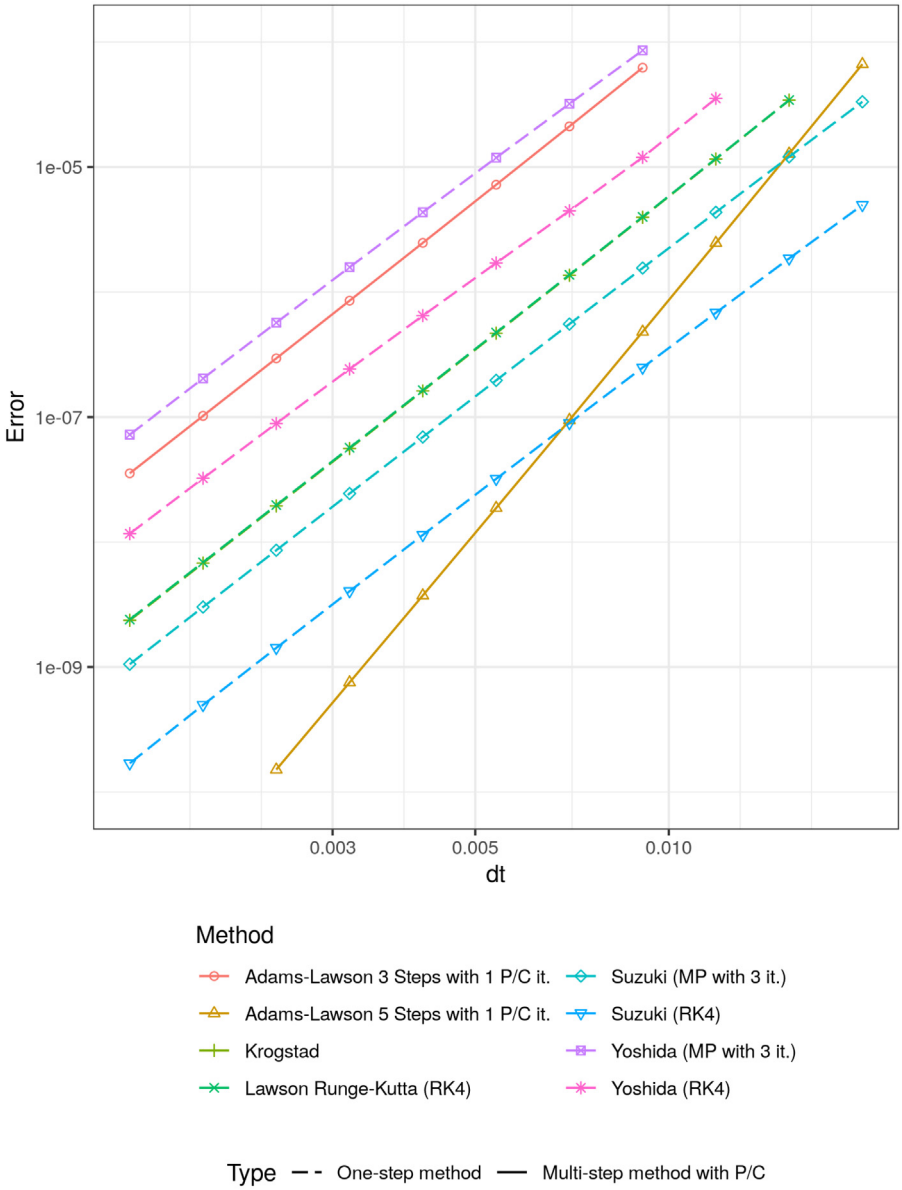

Fig. 3.7. Error by stepsize for the quantum dot, MCTDHF with $n = 6$.

The helium atom shown in Fig. 3.13, is solved for $t \in [0, 250]$ and $x \in [-512, 512]$ is discretized with 16384 Fourier modes. The time interval is chosen as sufficiently large to observe that almost constant stepsizes are restored after the pulse subsides. We observe that the chosen stepsizes are systematic, i.e., higher-order methods use larger time-steps, while the system is still at equilibrium. However, in the presence of the laser pulse, higher-order schemes react more strongly to the unsmoothness and choose smaller time-steps. We therefore stress that such an observation depends on the solution's smoothness, in the presence of very unsmooth data, lower order methods may be advantageous.

The same experiment is performed for the quantum dot for $t \in [0, 12]$, and $x \in [-20, 20]$ is discretized with 1024 Fourier modes, see Fig. 3.14. At the extrema of the energy functional, the behavior of the automatically chosen stepsizes becomes unsystematic in the sense that at some instances, higher-order schemes use smaller time steps. This seems to be related to stability issues, which restrict the stepsizes of higher-order methods more tightly.

3.8. Runtimes

We substantiate our claim that computation time for our 1D MCTDHF calculations is proportional to the number of evaluations of the nonlocal potential $\boldsymbol{B}$. In Figs. 3.15 and 3.16 we show the error (as controlled by the prescribed tolerances) compared to

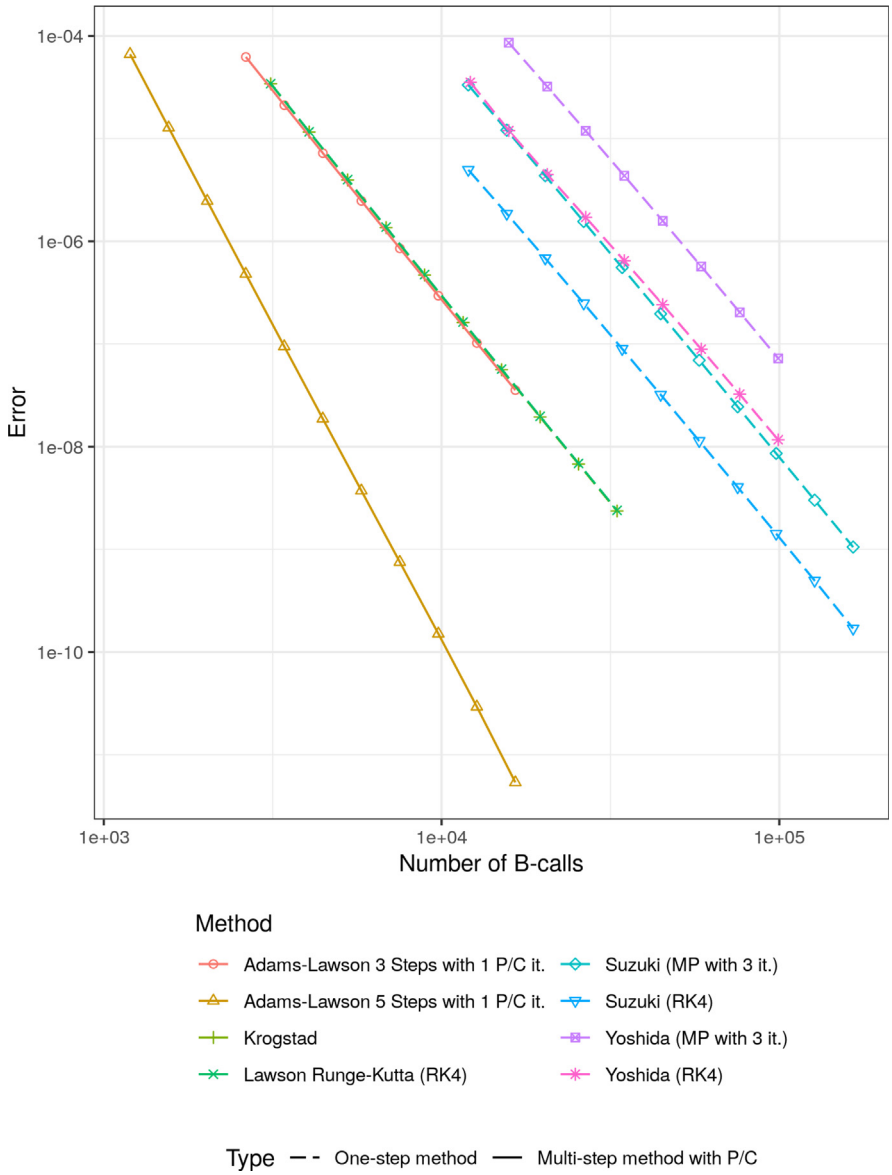

Fig. 3.8. Error by number of evaluations of B for the quantum dot, MCTDHF with $n = 6$.

a precise reference solution as before associated with the number of evaluations of B (represented by '•') and with required CPU time (represented by '×'). The computations are performed for the quantum dot (3.2) on the time interval $[0, 12]$. To increase the readability of the graphical representations below, we only investigate those methods that have been found to be stable in the previous investigations henceforth.

In Fig. 3.15, the results for MCTDHF with $n = 6$ are given, likewise in Fig. 3.16 for $n = 8$. Note that the former is the same experiment as in Fig. 3.12, and serves to demonstrate that the runtimes are indeed proportional to the number of evaluations of B. The earlier observation is corroborated that Adams–Lawson methods of higher order show the best performance. Moreover it is seen that here adaptivity yields a gain in computational efficiency over equidistant time-stepping by the same integrator (predictor/corrector multistep method of length $k + 1$) in addition to the benefit of reliability explained earlier by also showing the results for the same multistep methods on equidistant grids. Also, it is verified that as postulated, the computation time is proportional to the number of evaluations of B. The same conclusion can be drawn for both numbers of configurations.

To corroborate this observation, we give the computation times for some representative computations for the quantum dot (3.2) in Fig. 3.17, where $n = 8$ is chosen in MCTDHF and the CPU time in seconds is shown in relation to the number of evaluations of B. We select some representative methods from each class for this illustration.

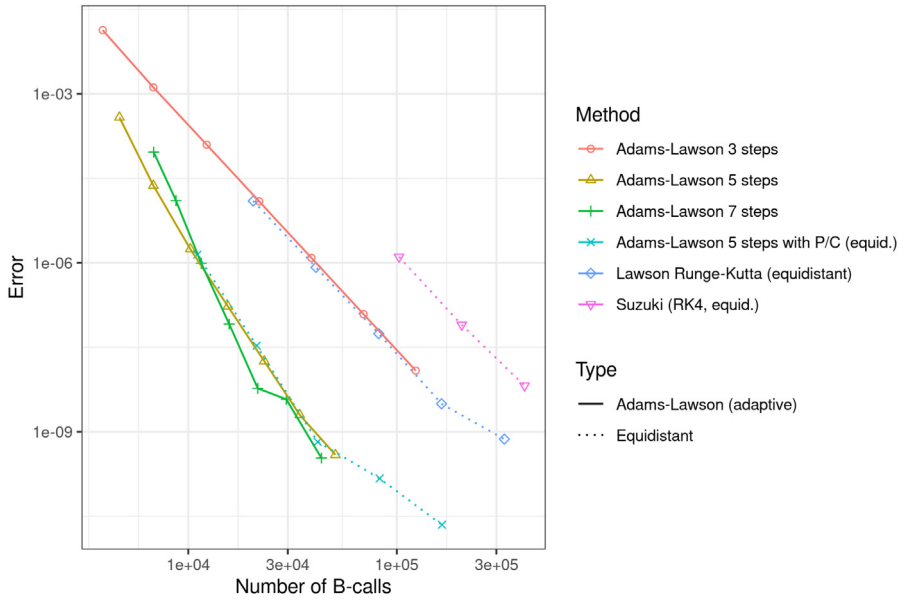

Fig. 3.9. Error by number of evaluations of B for helium, adaptive time-stepping, Adams–Lawson methods, MCTDHF with $n = 4$.

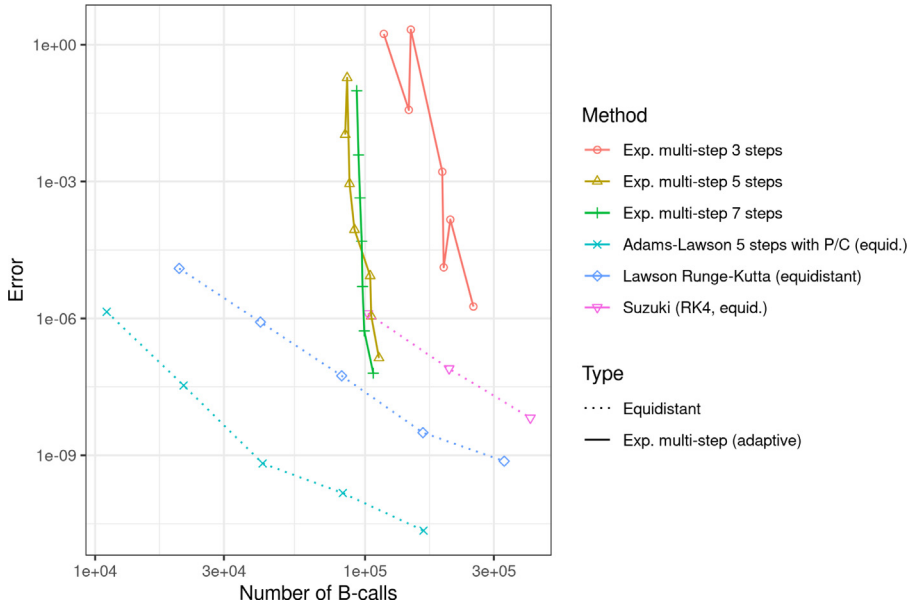

Fig. 3.10. Error by number of evaluations of B for helium, adaptive time-stepping, exponential multistep methods, MCTDHF with $n = 4$.

3.9. Achieved accuracy

In this subsection, we investigate the reliability of the adaptively achieved accuracy as compared to the prescribed tolerance. In Fig. 3.18, the ratio of achieved accuracy over prescribed tolerance is given for the helium atom for $t \in [0, 80]$ and $x \in [-256, 256]$ discretized with 8192 Fourier modes, Fig. 3.19 shows the same for the quantum dot on $t \in [0, 12]$ and $x \in [-20, 20]$ using 1024 Fourier modes. We observe that the exponential multistep methods, which have previously been found to be unstable, are also unreliable in this test, the tolerance is failed significantly.

The Lawson-type multistep methods are more reliable, the ratio is close to one, where it should be noted that the tolerance is reached more reliably for higher-order methods. The same observation also applies to the exponential multistep methods. Generally

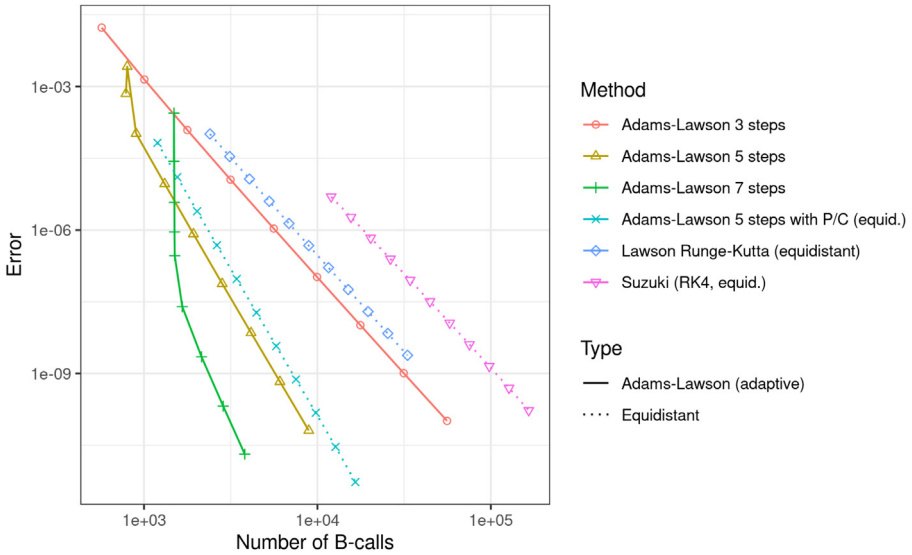

Fig. 3.11. Error by number of evaluations of B for the quantum dot, adaptive time-stepping, Adams–Lawson methods, MCTDHF with $n = 6$.

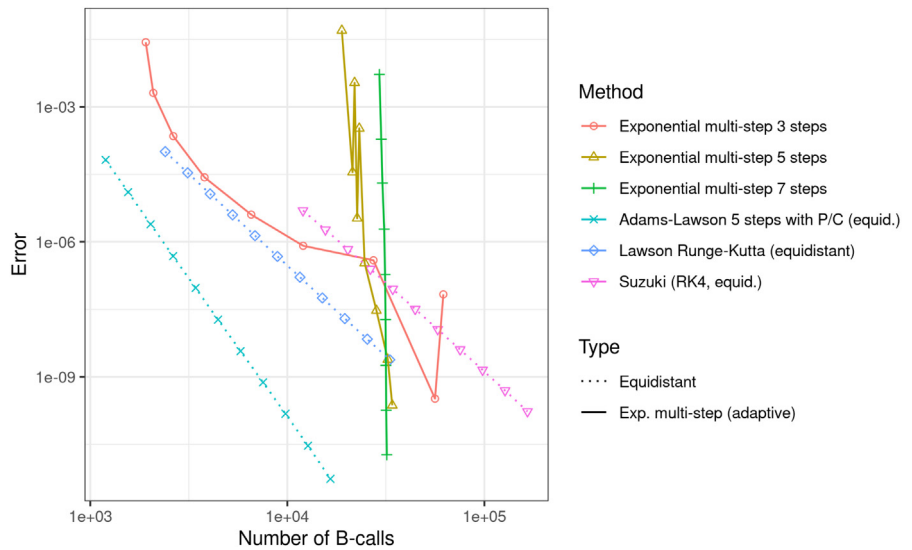

Fig. 3.12. Error by number of evaluations of B for the quantum dot, adaptive time-stepping, exponential multistep methods, MCTDHF with $n = 6$.

we conclude from this experiment that high-order adaptive Adams–Lawson methods serve to reach a tolerance very reliably and thus represent an efficient way to provide numerical solutions whose accuracy can be trusted.[2]

3.10. Tolerance-based stepsize variation

To illustrate the evolution of the stepsizes chosen automatically, we plot the stepsizes that are generated for different tolerances. We use an Adams–Lawson method of order five. We observe that stepsizes very consistently decrease with stricter tolerances.

For helium presented in Fig. 3.20 and again solved for $t \in [0, 80]$ and $x \in [-256, 256]$ (discretized at 8192 points), we observe two minima of stepsizes near the end of the integration interval for moderate tolerances. This seems to be related to a stability issue, as

[2] Note the logarithmic scaling in Figs. 3.18 and 3.19. The value of the monitored ratio is in fact larger throughout for the helium atom. Since it cannot be expected that local error control serves to control the global error exactly, the ratios which are of an order of magnitude up to 10^1 can be considered as reliable.

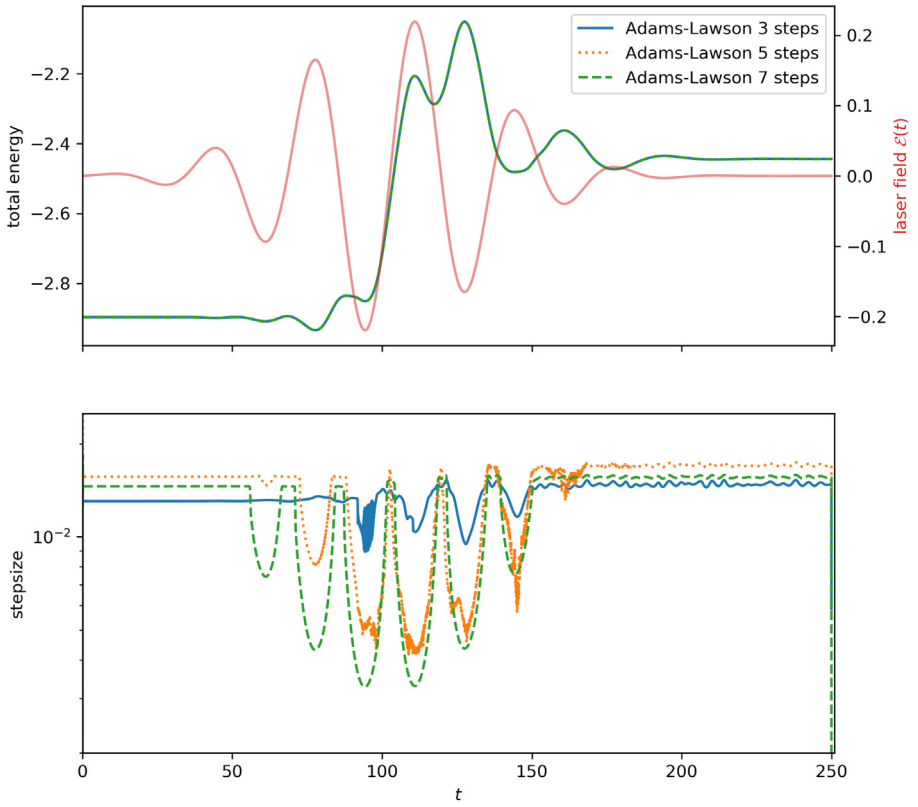

Fig. 3.13. Adaptive stepsizes for the helium atom compared to the smoothness of the laser field and the energy functional, adaptive time-stepping, MCTDHF with $n = 4$, Adams–Lawson multistep methods of different orders. The prescribed error tolerance is 10^{-5}.

the stepsizes in the minima are the same for all tolerances where the phenomenon is observed. For stricter tolerances, stepsizes are below these minima invariantly, so the phenomenon is not observed. For most of the time interval, an optimal stepsize is chosen and kept more or less constant.

For the quantum dot, the spatial discretization is again based on 1024 Fourier modes on $[-12, 12]$ and $t \in [0, 20]$. This example shows a stronger variation in the time-steps. This is due to the fact that for helium the laser field is weak until $t = 80$, whereas it is present from the start for the quantum dot. We observe in Fig. 3.21 that the choice of time-steps is consistent with the tolerance requirements, but for moderate tolerances the behavior becomes unsystematic in the extrema of the energy functional. Evidently, for moderate tolerances the stepsizes are too large to reflect reliable convergence behavior of the numerical approximation.

3.11. Convergence of the MCTDHF approximation

We demonstrate that our choice of the number of orbitals n is meaningful, by comparing the approximations computed by the adaptive Adams–Lawson four-step predictor/corrector method for different n for (3.1) on the time interval $t \in [0, 12\pi/\omega]$ (the spatial discretization again uses 16384 points). We apply MCTDHF with $n = 2, 4, 6, 8, 10$ and plot in Fig. 3.22 the total energies and the external field $\mathcal{E}(t)$ (top panel), the differences between the approximations for $n = 2$, $n = 4$, $n = 6$ and $n = 8$ and the solution for $n = 10$ (middle panel) and the automatically chosen stepsizes (bottom panel) for tolerance 10^{-5}. We observe in the top panel that the approximations of the energies approach the energy for $N = 10$, for $N = 2$ the energy deviates significantly, while the energies computed for $N = 6$ and $N = 8$ are very close to that for $N = 10$. This is emphasized in the logarithmic plot of the energy differences in the middle panel. The bottom panel shows smaller step-sizes for larger N while the dynamics are smooth, and a drastic reduction in the timesteps for unsmooth dynamics, with the most significant effect for N small.

4. Conclusions

We have investigated the performance of exponential integrators for the time integration of the equations of motion associated with the MCTDHF equations for model problems in one spatial dimension. It was found that explicit Runge–Kutta methods, but

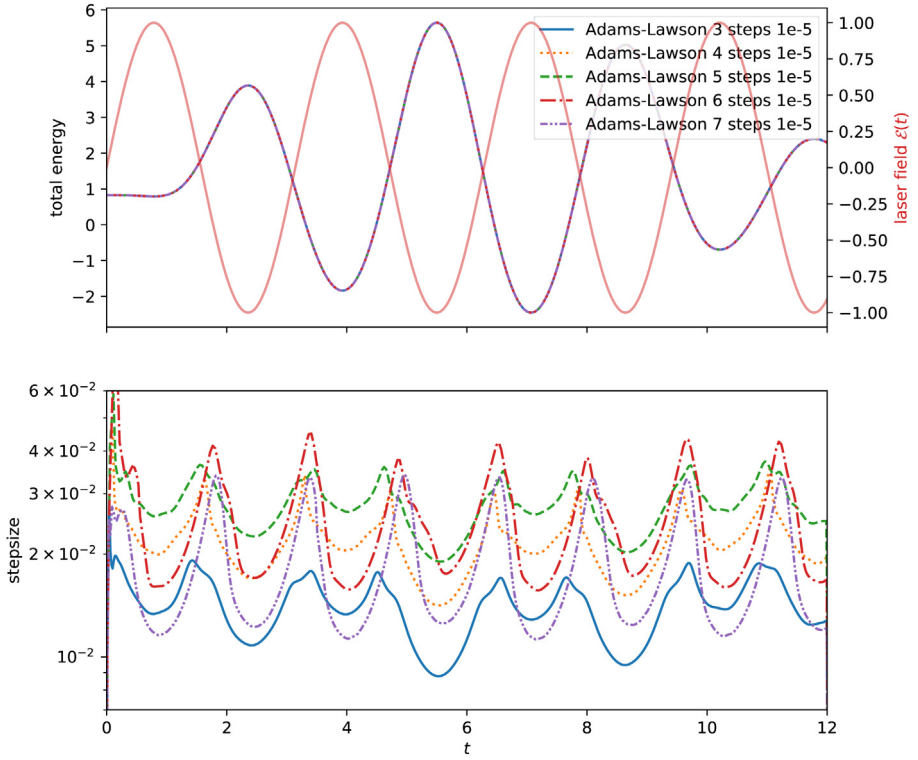

Fig. 3.14. Adaptive stepsizes for the quantum dot (3.2) compared to the smoothness of the laser field and the energy functional, adaptive time-stepping, MCTDHF with $n = 6$, Adams–Lawson multistep methods of different orders. The prescribed error tolerance is 10^{-5}.

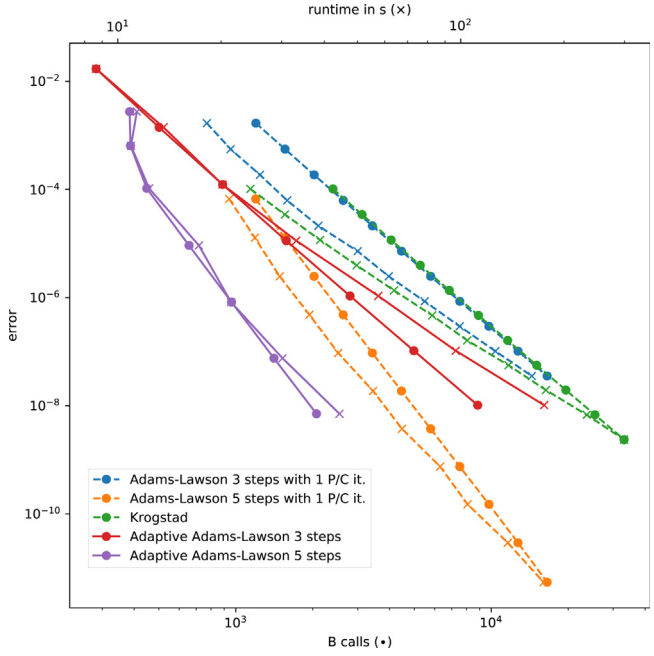

Fig. 3.15. Error by number of evaluations of B ('•') and by computation time ('×') for the quantum dot (3.2), adaptive time-stepping, Adams–Lawson methods, MCTDHF with $n = 6$. Adams–Lawson P/C methods and Krogstad method on equidistant grids given for comparison.

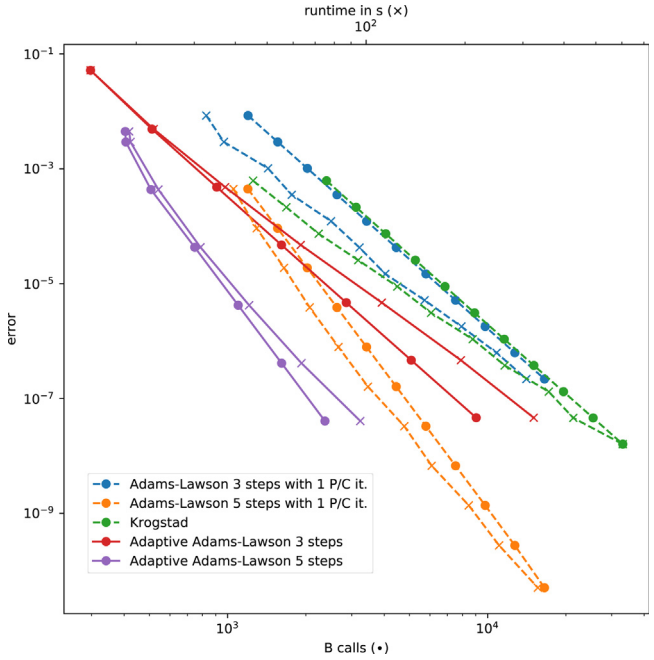

Fig. 3.16. Error by number of evaluations of B ('•') and by computation time ('×') for the quantum dot (3.2), adaptive time-stepping, MCTDHF with $n = 8$. Adams–Lawson P/C methods and Krogstad method on equidistant grids given for comparison.

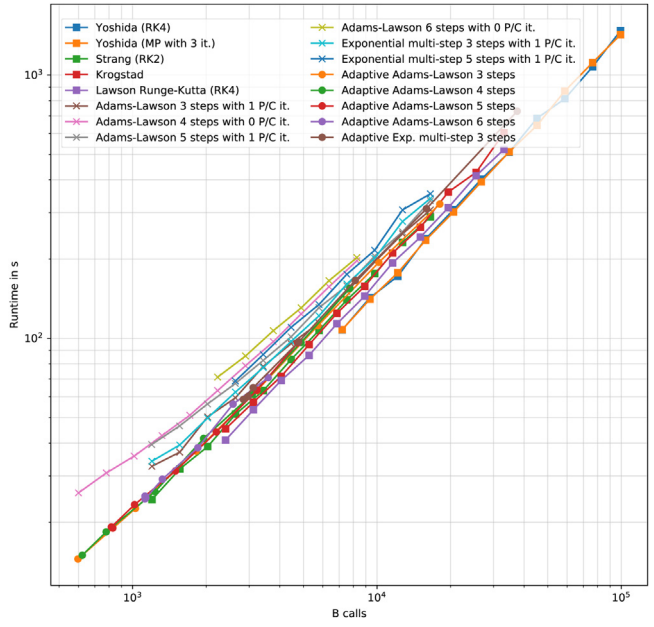

Fig. 3.17. Relationship between runtime and number of evaluations of B for the quantum dot (3.2), MCTDHF with $n = 8$.

also exponential multistep methods are unstable in the sense that they fail even to preserve the norm of the solution. Splitting methods and exponential Runge–Kutta methods are stable, and so are Lawson Runge–Kutta methods. For Adams–Lawson multistep methods this holds in general only when one corrector step is performed. For the stable integrators, the convergence order and computational efficiency was investigated, where the latter compares the achieved accuracy with the number of evaluations of the

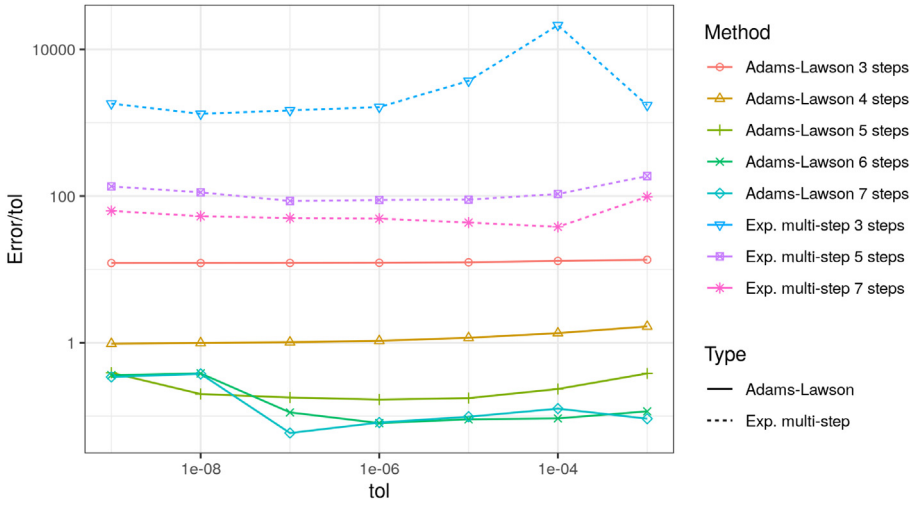

Fig. 3.18. Ratio of the achieved error vs. the prescribed tolerance for the helium atom (3.1), MCTDHF with $n = 4$.

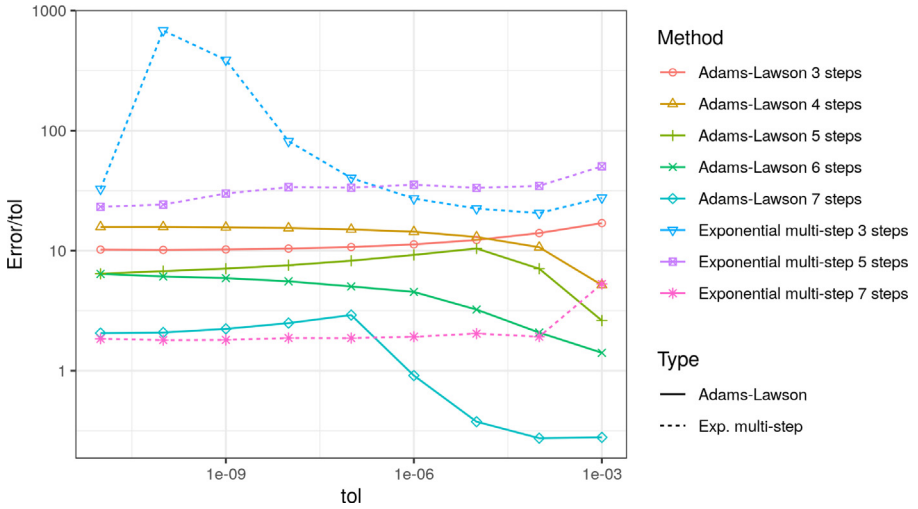

Fig. 3.19. Ratio of the achieved error vs. the prescribed tolerance for the quantum dot (3.2), MCTDHF with $n = 6$.

nonlocal potential terms, which in the present setting induces a large computational effort. The stable methods show their expected convergence orders, and high-order multistep methods are most efficient for very high demands on the solution accuracy.

Adaptive choice of the time-steps may increase the computational efficiency, but foremostly it guarantees that a prescribed tolerance is achieved reliably, without the necessity of guessing appropriate stepsizes a priori, and at moderate additional cost. Indeed, the achieved accuracy corresponds well with the prescribed requirement in the case of Lawson multistep methods, and the automatically chosen stepsizes reflect the solution's local smoothness.

Declaration of competing interest

The authors declare that they have no known competing financial interests or personal relationships that could have appeared to influence the work reported in this paper.

Acknowledgments

The authors would like to acknowledge support by the Vienna Science and Technology Fund (WWTF) under grant MA14-002. The computations have been conducted on the Vienna Scientific Cluster (VSC).

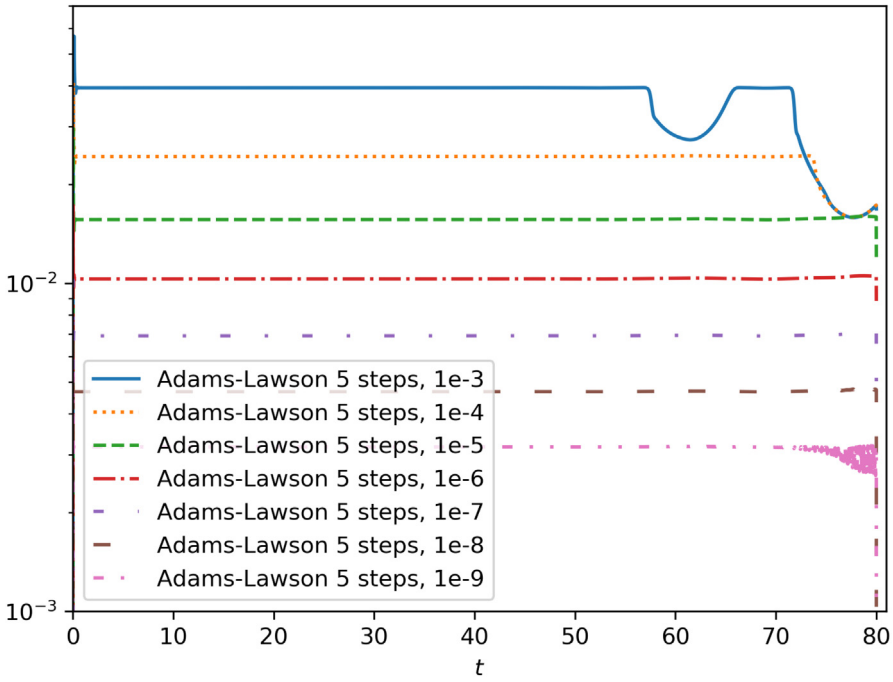

Fig. 3.20. Variation of stepsizes for several prescribed tolerances for the helium atom (3.1), MCTDHF with $n = 4$.

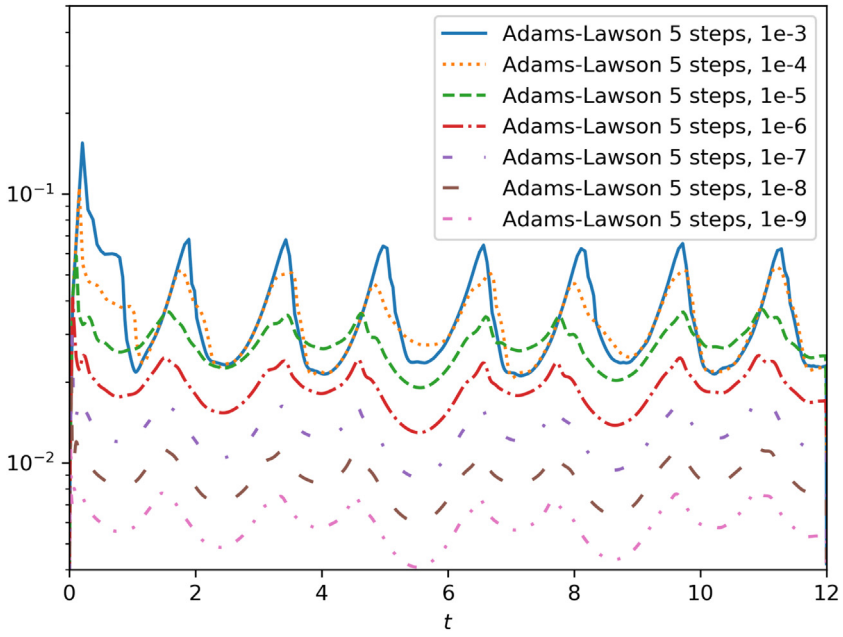

Fig. 3.21. Variation of stepsizes for several prescribed tolerances for the quantum dot (3.2), MCTDHF with $n = 6$.

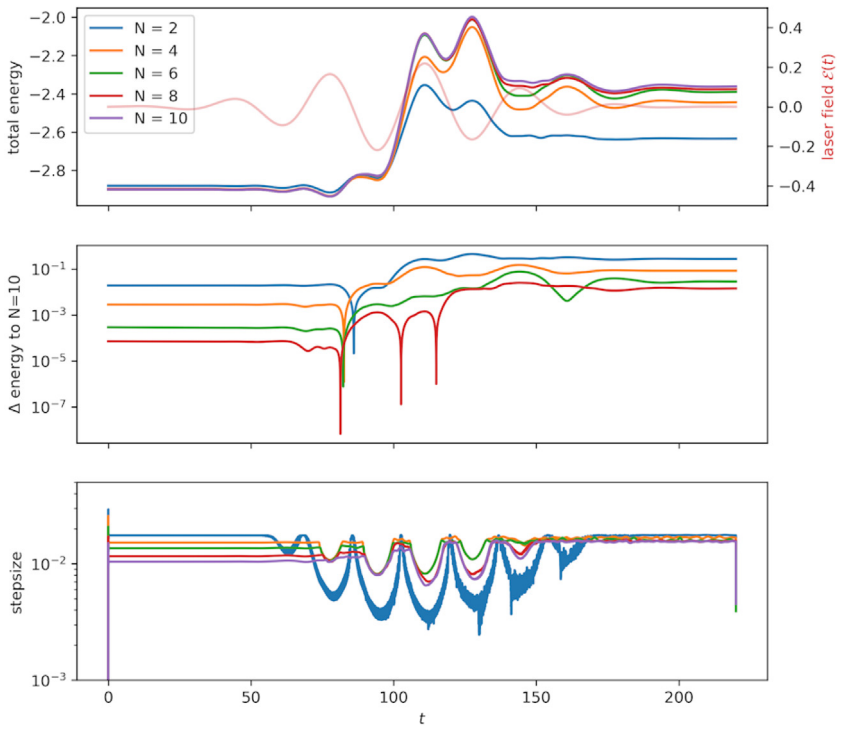

Fig. 3.22. MCTDHF with $n = 2, 4, 6, 8, 10$ applied to (3.1). Total energies and the external field $\mathcal{E}(t)$ (top panel), the differences between these approximations (middle panel) and the automatically chosen stepsizes (bottom panel), computed with Adams–Lawson four-step adaptive method.

References

[1] Alon O, Streltsov A, Cederbaum L. Multiconfigurational time-dependent Hartree method for bosons: Many-body dynamics of bosonic systems. Phys Rev A 2008;77:033613.
[2] Kato T, Kono H. Time-dependent multiconfiguration theory for electronic dynamics of molecules in an intense laser field. Chem Phys Lett 2004;392:533–40.
[3] Zanghellini J, Kitzler M, Fabian C, Brabec T, Scrinzi A. An MCTDHF approach to multi-electron dynamics in laser fields. Laser Phys 2003;13(8):1064–8.
[4] Hochstuhl D, Hinz C, Bonitz M. Time-dependent multiconfiguration methods for the numerical simulation of photoionization processes of many-electron atoms. Eur Phys J Spec Top 2014;223(2):177–336. http://dx.doi.org/10.1140/epjst/e2014-02092-3.
[5] Sato T, Ishikawa KL. Time-dependent complete-active-space self-consistent-field method for multielectron dynamics in intense laser fields. Phys Rev A 2013;88:023402.
[6] Sato T, Ishikawa K, Březinová I, Lackner F, Nagele S, Burgdörfer J. Time-dependent complete-active-space self-consistent-field method for atoms: Application to high-order harmonic generation. Phys Rev A 2016;94:023405.
[7] Stoer J, Bulirsch R. Introduction to numerical analysis, 12 of texts in applied mathematics. New York: Springer Verlag; 1993.
[8] Auzinger W, Grosz A, Hofstätter H, Koch O. Adaptive exponential integrators for MCTDHF. In: Lirkov SMI, editor. Large-scale scientific computing. 11958 of Lecture notes in computer science, Springer Verlag; 2020, p. 557–65.
[9] Antoine X, Bao W, Besse C. Computational methods for the dynamics of the nonlinear Schrödinger/Gross–Pitaevskii equations. Comput Phys Comm 2013;184:2621–33.
[10] Chang Q, Jia E, Sun W. Difference schemes for solving the generalized nonlinear Schrödinger equation. J Comput Phys 1999;148:397–415.
[11] Bao W, Tang Q, Xu Z. Numerical methods and comparison for computing dark and bright solitons in the nonlinear Schrödinger equation. J Comput Phys 2013;235:423–45.
[12] Auzinger W, Březinová I, Hofstätter H, Koch O, Quell M. Practical splitting methods for the adaptive integration of nonlinear evolution equations. Part II: Comparisons of local error estimation and step-selection strategies for nonlinear Schrödinger and wave equations. Comput Phys Comm 2019;234:55–71.
[13] Donsa S, Hofstätter H, Koch O, Burgdörfer J, Březinová I. Long-time expansion of a Bose–Einstein condensate: Observability of Anderson localization. Phys Rev A 2017;96.
[14] Hairer E, Lubich C, Wanner G. Geometric numerical integration. Berlin–Heidelberg–New York: Springer-Verlag; 2002.
[15] Jahnke T, Lubich C. Error bounds for exponential operator splittings. BIT 2000;40:735–44.
[16] Thalhammer M. Convergence analysis of high-order time-splitting pseudo-spectral methods for nonlinear Schrödinger equations. SIAM J Numer Anal 2012;50:3231–58.
[17] Lubich C. On splitting methods for Schrödinger–Poisson and cubic nonlinear Schrödinger equations. Math Comp 2008;77:2141–53.
[18] Koch O, Lubich C. Variational splitting time integration of the MCTDHF equations in electron dynamics. IMA J Numer Anal 2011;31:379–95.
[19] Koch O, Neuhauser C, Thalhammer M. Error analysis of high-order splitting methods for nonlinear evolutionary Schrödinger equations and application to the MCTDHF equations in electron dynamics. M2AN Math Model Numer Anal 2013;47:1265–84.
[20] Hersch J. Contribution à la méthode des équations aux différences. Z Angew Math Phys 1958;9:129–80.
[21] Hochbruck M, Lubich C, Selhofer H. Exponential integrators for large systems of differential equations. SIAM J Sci Comput 1998;19:1552–74.
[22] Hochbruck M, Ostermann A. Exponential integrators. Acta Numer 2010;19:209–86.
[23] Minchev P, Wright W. A review of exponential integrators for first order semi-linear problems. Tech. rep. 2/2005, Trondheim, Norway: NTNU – Norwegian University of Science and Technology; 2005.

[24] Niesen J, Wright W. Algorithm 919: A Krylov subspace algorithm for evaluating the φ-functions appearing in exponential integrators. ACM Trans Math Softw 2012;38:22.
[25] Friedli A. Verallgemeinerte Runge–Kutta verfahren zur lösung steifer differentialgleichungssysteme. In: Bulirsch R, Grigorieff G, Schröder J, editors. Numerical treatment of differential equations. 631 of Lecture notes in mathematics, Springer; 1978, p. 35–50.
[26] Hochbruck M, Ostermann A. Exponential Runge–Kutta methods for parabolic problems. Appl Numer Math 2005;53:323–39.
[27] Luan V, Ostermann A. Exponential B-series: The stiff case. SIAM J Numer Anal 2013;51:3431–45.
[28] Liang X, Khaliq A, Sheng Q. Exponential time differencing Crank–Nicolson method with a quartic spline approximation for nonlinear Schrödinger equations. Appl Math Comput 2014;235:235–52.
[29] Montanelli H, Bootland N. Solving periodic semilinear stiff PDEs in 1D, 2D and 3D with exponential integrators. preprint Available from: http://arxiv.org/abs/1604.08900v3.
[30] Krogstad S. Generalized integrating factor methods for stiff PDEs. J Comput Phys 2005;203:72–88.
[31] Calvo M, Palencia C. A class of explicit multistep exponential integrators for semilinear problems. Numer Math 2011;102:367–81.
[32] Hochbruck M, Ostermann A. Exponential multistep methods of adams type. BIT 2011;51:889–908.
[33] Hochbruck M, Ostermann A, Schweitzer J. Exponential Rosenbrock–type methods. SIAM J Numer Anal 2009;47:786–803.
[34] Ostermann A, Thalhammer M, Wright W. A class of explicit exponential general linear methods. BIT 2006;46:409–31.
[35] Auzinger W, Łapińska M. Convergence of rational multistep methods of Adams–padé type. BIT 2012;52:3–20.
[36] Lawson J. Generalized Runge–Kutta processes for stable systems with large Lipschitz constants. SIAM J Numer Anal 1967;4:372–80.
[37] Hult J. A fourth-order Runge–Kutta in the interaction picture method for simulating supercontinuum generation in optical fibers. J Lightwave Technol 2007;25:3770–5.
[38] Balac S, Fernandez A, Mahé F, Méhats F, Texier-Picard R. The interaction picture method for solving the generalized nonlinear Schrödinger equation in optics. M2AN Math Model Numer Anal 2016;50:945–64.
[39] Hochbruck M, Leibold J, Ostermann A. On the convergence of Lawson methods for semilinear stiff problems. Numer Math 2020;145:553–80.
[40] Balac S, Mahé F. Embedded Runge–Kutta scheme for step-size control in the interaction picture method. Comput Phys Comm 2013;184:1211–9.
[41] Dormand J, Prince P. A family of embedded Runge–Kutta formulae. J Comput Appl Math 1980;6:19–26.
[42] Cano B, González-Pachón A. Projected explicit lawson methods for the integration of Schrödinger equation. Numer Methods Partial Differential Equations 2015;31:78–104.
[43] Koch O, Neuhauser C, Thalhammer M. Embedded split-step formulae for the time integration of nonlinear evolution equations. Appl Numer Math 2013;63:14–24.
[44] Balac S, Fernandez A. SPIP: A computer program imlementing the interaction picture method for the simulation of light-wave propagation in optical fibers. Comput Phys Comm 2016;199:139–52.
[45] Whalen P, Brio M, Moloney J. Exponential time-differencing with embedded Runge–Kutta adaptive step control. J Comput Phys 2015;280:579–601.
[46] Koch O. Convergence of exponential lawson-multistep methods for the MCTDHF equations. M2AN Math Model Numer Anal 2019;53:2109–19. http://dx.doi.org/10.1051/m2an/2019033.
[47] Caillat J, Zanghellini J, Kitzler M, Kreuzer W, Koch O, Scrinzi A. Correlated multielectron systems in strong laser pulses — an MCTDHF approach. Phys Rev A 2005;71:012712.
[48] Zanghellini J, Kitzler M, Brabec T, Scrinzi A. Testing the multi-configuration time-dependent Hartree-Fock method. J Phys B: At Mol Phys 2004;37:763–73.
[49] Dirac P. Note on exchange phenomena in the Thomas atom. Proc Cambridge Philos Soc 1930;26:376–85.
[50] Frenkel J. Wave mechanics. In: Advanced general theory. Oxford: Clarendon Press; 1934.
[51] Hairer E, Nørsett S, Wanner G. Solving ordinary differential equations I. Berlin–Heidelberg–New York: Springer-Verlag; 1987.
[52] Press W, Flannery B, Teukolsky S, Vetterling W. Numerical recipes — the art of scientific computing. Cambridge, U.K.: Cambridge University Press; 2007.